Pick and Place Simulation of Parallel End Effector Grasping Fruits
Final Project Report

Jessica Anz, Trevor Oshiro

Abstract— A simulated model of a parallel end-effector grasping a piece of fruit was developed for force testing and end-effector design. This model consists of a 2D simulation of 2 soft elastic beams linearly closing over a piece of fruit. The modified mass method algorithm is used for contact forces between the gripper and the fruit. Beam deformations as well as contact forces between the beam and fruit are calculated and visualized through the simulation.

I. INTRODUCTION

The usage of robotics to automate the agricultural industry is a developing field. A key element of automating crop harvesting is the picking up and placing of various crops. This is a complex task to automate, as the amount of force applied to the crop has to be precise enough to grasp the crop without damaging it [1]. In order to test various forces applied to various crops, a simulation model is needed. This project shall develop a simulation that can be used to test different forces applied to a fruit model.

II. PROJECT OBJECTIVES

The primary objective of this project is to develop a simulated model of the robotic harvesting of a piece of fruit. This model should be composed of a parallel end effector which closes in on the piece of fruit in a linear motion [2]. This model should accurately simulate the contact forces between the robot gripper and the fruit. It should also predict the fruit deformation caused by applied forces [3]. This simulation shall be developed in a 3 stage process. The first stage will create a 2D simplified model of a gripper closing on a circular fruit model. The second stage will further this model by adding complexities to both the gripper and fruit geometries. The final stage will expand this simulation into a 3D model if possible, however the majority of analysis will be done on the model from stage 2. The final simulation should facilitate the analysis of forces from a soft gripper geometry applied to a fruit. This will help prevent the crushing and dropping of fruits in real world robotic harvesting applications, which will improve the quality and efficiency of harvesting [4].

III. CONTACT ALGORITHM

The initial main focus of this project was the implementation of an algorithm to efficiently handle contact between surfaces of varying geometries. Methods such as the Implicit Contact Model and Incremental Potential Contact Model were considered. Both of these methods effectively implement simulation of contact through the calculation of contact energy, and they would be able to simulate frictional contact

between surfaces [5] [6]. However, due to time constraints, the project scope was narrowed to the analysis of contact forces generated between objects, so the simulation model was simplified to contact between a rigid object (the agricultural product) and a flexible component (the prongs of the gripper). Analysis of friction would be closely related with the contact forces between the objects, so this simplification acceptable for the purposes of this project.

Under these considerations, the model for contact chosen was the modified mass method. Through the manipulation of mass within the time-stepping loop, the method effectively applies an artificial change in speed for nodes in contact. The following equation was implemented for the equation of motion:

$$\frac{1}{\Delta t}\left[\frac{q(t_{k+1})-q(t_k)}{\Delta t}-u(t_k)\right]-\frac{1}{m_i}Sf-z=0 \qquad (1)$$

By utilizing the S matrix and z vectors generated through each collision detection iteration, equation 1 was applied to modify mass values with S and change in velocity with z to effectively can handle complex curvatures during contact. Implementation within our script was inspired by the paper by Baraff and Witkin, whom implement this algorithm to simulate the contact between cloth and other rigid objects [7].

To ensure proper implementation of the method, it was first applied to a simple case of one node bouncing on a horizontal surface. In this case the directions of constraint would be solely within the y-direction of the simulation, and the "bounce" would be generated from the change in velocity between prediction and correction steps taken by the method. Because the change in velocity was generated between different iterations of calculations for position, challenges arose in obtaining consistent results in the change in velocity upon contact with the surface. Figure 1 shows inconsistencies in the method, significant spikes in the calculation in the change of velocity can be seen.

To alleviate this problem within the simulation, a solution generated was the implementation of smaller time-steps in the simulation when the objects are within a certain proximity of each other. When the contact detection portion of the code loops through the nodes, an additional flag was added to indicate the close proximity of nodes during the simulation. Upon detection, a separate loop would iterate over a smaller time-step to reduce chances of spikes in the calculated velocity for instances. The time-step would then revert to the larger time-step when further away from the contact surface. With the implementation of this method, the
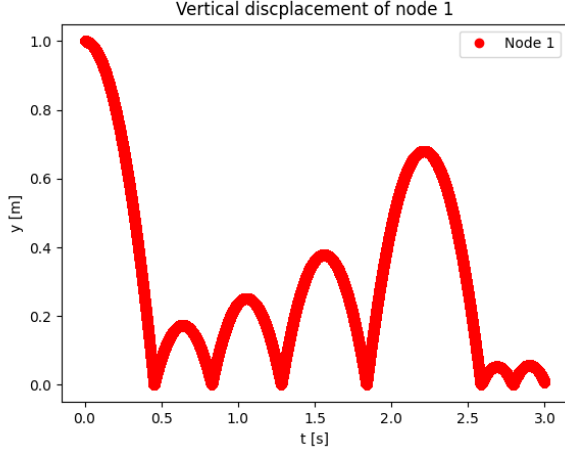
Fig. 1: Inconsistent bouncing from a time step of $1e-4s$ time step application
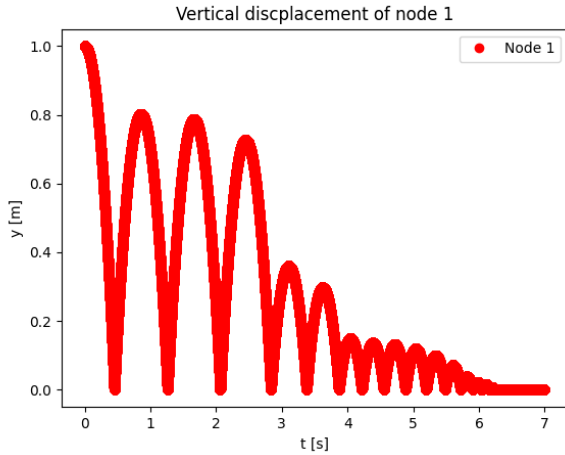
following plot in figure 2 was generated.

Fig. 2: More consistent results from contact with smaller a smaller time-step

The tapering of the bounce amplitude from figure 2 shows better consistency within the contact. Figure 2 also uses a time-step of $1e-5s$ and $1e-6s$ when detected as close to the surface for contact. As future implementations of this methods involved multiple nodes, it was important to address this potential issues to avoid the model potentially breaking during the simulation run. If the contact produced the sudden spike in velocity, the deformation of the nodes would then deviate significantly from what would be expected.

Similarly, the consistency of the contact would be especially important when considering the reaction force values calculated. Reaction forces were calculated with a separate equation shown below:

$$R_f = \frac{m}{\Delta t}\left[\frac{q(t_{k+1})-q(t_k)}{\Delta t} - u(t_k)\right] - f \quad (2)$$

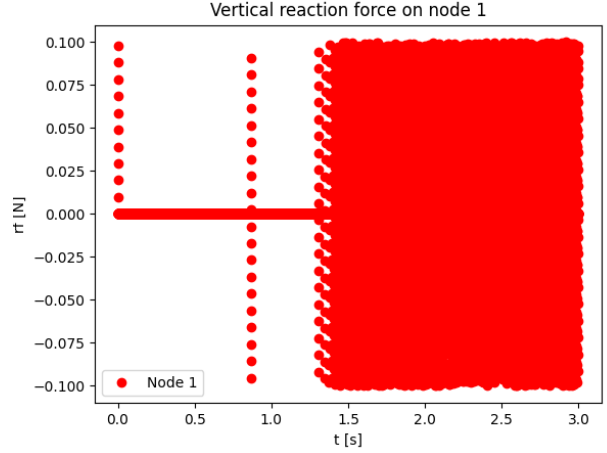As shown with figure 3, issues were present with the calculation of the reaction force.

Fig. 3: Variations in reaction force calculated within contact

These issues were primarily due to an implementation issue of the method, along with the larger time-steps introducing variations in the results.

In order to verify that the modified mass method algorithm was working correctly, the algorithm was implemented in a basic simulation of a single node bouncing off a sinusoidal surface. This simulation proves that the algorithm is correctly calculating the normal vector at the point of contact and using that vector. Intuitively, the ball is expected to fall and bounce off the sinusoidal surface at an angle normal to the surface. The implemented simulation matched intuition, providing another check that the modified mass method was working.
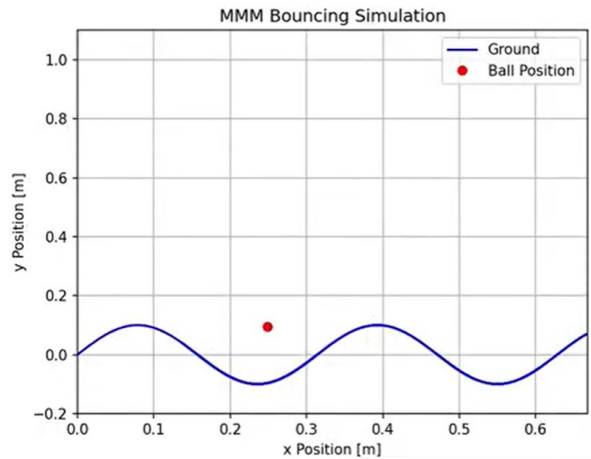

Fig. 4: Modified Mass Method Bouncing Simulation

IV. CONTACT OF ELASTIC BEAMS

Upon the verification of the Modified Mass method, the next stage of the project was to implement the contact across a greater number of nodes. This phase of the project

then shifted to model a string of nodes as an elastic beam. Each of the nodes would be modeled as mass connected with compression/tension springs between nodes, along with torsional springs every three nodes to simulate bending. Because the simulation was simplified to a 2D environment, the effects of twisting of the nodes was not considered in the simulation [8]. The material properties of the gripper were further simplified in the simulation, where a constant, representative value of modulus of elasticity was chosen. Along with the above considerations, the following were also applied within this stage of the project:

1) $F_C = 0$: The gripper would operate in the air, so there would be negligible viscosity.
2) $u_{gripper} = 0$: The gripper prongs would initially be at rest before grasping
3) $a_{grasp} = c$: The gripper grasp would have a constant horizontal acceleration to simulate a parallel end-effector
4) $a_{weight} = -g$: The end effector would be mid-air, so the gripper prongs would have gravity effects applied
5) $E_{gripper} = 1MPa$: The chosen value for elasticity to simulate soft rubbers
6) Rectangular cross section of $2cm$ x $1cm$ to resemble geometries of currently used grippers

To simulate the end-effector grasping movement, boundary conditions would be applied within the first two nodes. These nodes would only be impacted from a_{grasp}, so they would be excluded from impacts of elastic forces between beams in the simulation loop. When testing the grasping movement of the gripper, the value of a_{grasp} was set to be the acceleration of gravity as a benchmark value. The rest of the end-effector loop would be left free. Figure 5 shows the diagram used to represent the model being simulated within this phase.
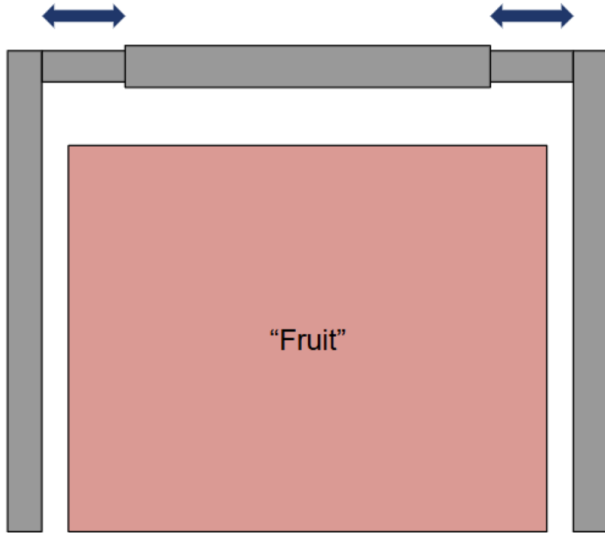

Fig. 5: Diagram of simulated model for flat surface

To iterate between different geometries, the node number chosen for this portion of the project was chosen to be

10. From the initial tuning of the contact algorithm, the consistency between the change in velocity applied and oscillations in node positions were behaviors evident within the simulation. Especially within simulations involving multiple nodes, oscillations of nodal positions between iterations of the predictor and corrector loop of the modified mass method would potentially make nodes "stuck" in a position through repeated oscillation close to points of contact. Under these considerations, 10 nodes were used within trials for the elastic beam simulations. This number would provide representative shapes of the gripper prongs, while also keeping the points of contact within the beam minimal. A smaller time-step based on proximity was also applied in these trials. Sample plots of contact between the beam and a flat surface are shown within figures 6, 7, and 8.
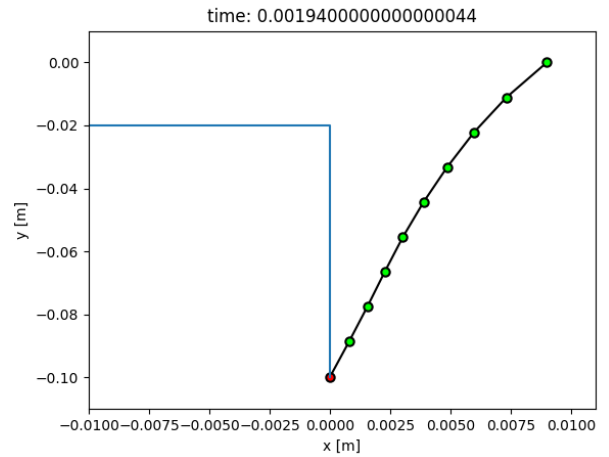

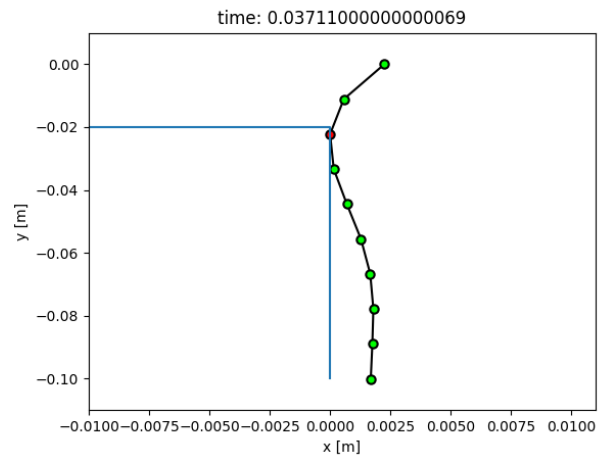Fig. 6: Contact between flat surface and node 10

Fig. 7: Contact between flat surface and node 3

within figures 6, 7, and 8, a parabola was chosen to model the curve in the gripper prong. Each of the figures also indicated where contact and reaction force values were most significant through the red color of the gripper prong's node.
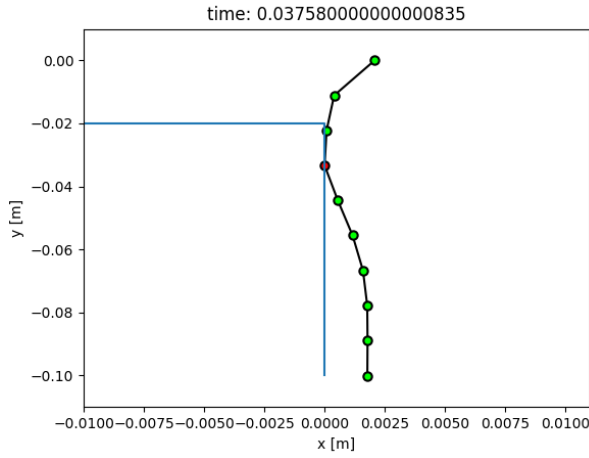
Fig. 8: Contact between flat surface and node 4

As seen between figures 7 and 8, a change in acceleration in the surface contact causes a rebound of node 3 as node 4 came into contact. Further research into modeling contact and material properties of the rubbers in the gripper may be needed to verify this behavior to be representative for the simulation.

Upon completion of the simulation, the reaction force magnitudes were plotted within figure 9.
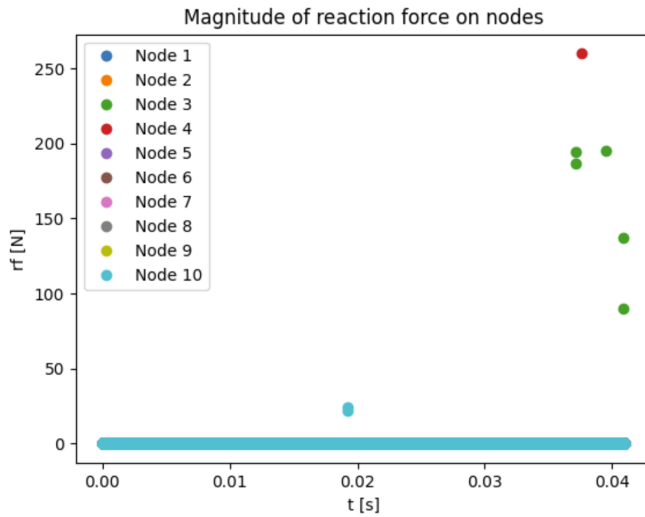

Fig. 9: Plot of reaction forces present in the contact simulation

Figure 9 indicates the magnitude of the reaction forces present for each of the nodes, and it shows corresponding peaks for the contacts present within figures 6, 7, and 8. As the magnitude of the reaction forces plotted was significantly higher than expected, the frequency and relative magnitude of the values may be more representative when analyzing the overall behavior of the gripper during the grasping task. Thus, nodes 3 and 4 would be considered as critical points along the gripper that need to be analyzed during

the design process. As points showing the highest reaction force magnitude present and the most frequent collisions, they would be the points under the most stress from contact with the fruit object and exert the most force in the process.

V. COLLISIONS WITH CURVED SURFACES

With implementation of the gripper for flat surfaces, the next iteration of the simulation would be applications to surfaces of varying geometries. The simplest model for a fruit that still retains a reasonable level of accuracy would be a circle. Therefore, a circle was chosen to model the fruit in the robot gripper. In order to detect collisions with this fruit model, brute force collision detection was used. This involved defining the position of the circle as centered within the gripper. Then the position of each node with respect to the fruit circle was calculated. If the node's position passed the outline of the circle then a collision was triggered and the node was set back onto the outline of the circle. Pseudocode to clarify the implementation of collision detection is provided below.

Algorithm 1 Collision Test Function

1: **Input:**
2:     $\mathbf{q}_{\text{test}}$ ▷ Node positions

3: **Initialize:**
4:     $\mathbf{q}_{\text{con}} \leftarrow \mathbf{q}_{\text{test}}$ ▷ Initialize constrained positions
5:     $\mathbf{con}_{\text{ind}} \leftarrow 0$ ▷ Constrained node indices
6:     $\mathbf{free}_{\text{ind}} \leftarrow 0$ ▷ Free node indices
7:     $\mathbf{mat} \leftarrow \mathbf{0}$ ▷ Matrix for constraint conditions
8:     $radius, \; center_x, \; center_y$ ▷ Circle parameters

9: **for** i in *nodes* **do**

10:     **Define Circle:**
11:         $\text{circle}_x \leftarrow \text{circle(parameters)}$
12:         $\text{circle normal} \leftarrow \text{circle normal vector(parameters)}$

13:     **Check for Collision:**
14:     **if** $\text{circle}_x \neq \text{None}$ **and** $\text{node}_x > \text{circle}_x$ **then**

15:             $\text{node}_x \leftarrow \text{circle}_x$ ▷ Constrain position to circle
16:             $\mathbf{mat}[i] \leftarrow \begin{bmatrix} \text{circle normal}[0] & \text{circle normal}[1] & 0 \\ 0 & 0 & 0 \end{bmatrix}$
17:             $\mathbf{con}_{\text{ind}}[i] \leftarrow i$
18:     **else**
19:             $\mathbf{free}_{\text{ind}}[i] \leftarrow i$
20:             $\mathbf{mat}[i] \leftarrow \mathbf{0}$ ▷ No constraint
21:     **end if**
22: **end for**

23: **Update Indices:**
24: $\mathbf{con}_{\text{ind}} \leftarrow \text{Update}$
25: $\mathbf{free}_{\text{ind}} \leftarrow \text{Update}$

26: **Return:** $\mathbf{con}_{\text{ind}}, \mathbf{free}_{\text{ind}}, \mathbf{q}_{\text{con}}, \mathbf{mat}$

Once the circle had been properly defined as a collision obstacle, the simulation could be tested. A fruit radius of 5 cm was used to model a small apple or a tangerine. All other simulation parameters were kept consistent with that of the previous model. Results of the simulation are plotted below. As seen in figure 10, the prongs of the gripper approach the surface of the fruit and start to curve slightly as they come into contact with the fruit.
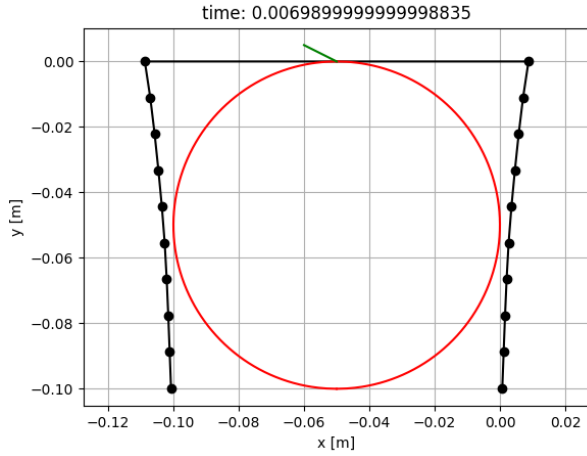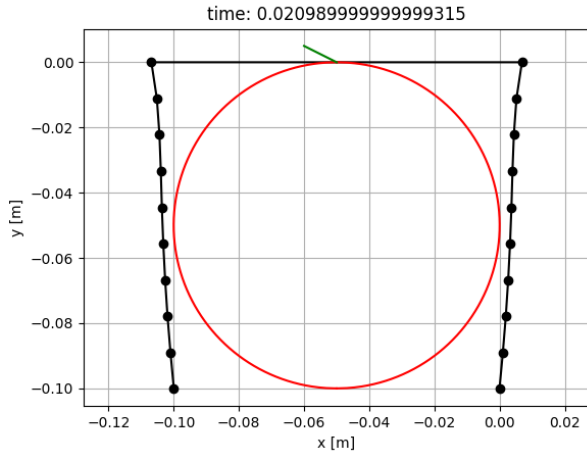

Fig. 10: Curved Fruit Implementation 1

Fig. 11: Curved Fruit Implementation 2

From the simulation, results for the magnitude of the reaction force were obtained. As seen in figure 14, the reaction force reached a maximum magnitude of approximately 250 N, which is similar to the results obtained with the rectangular shaped fruit. There is also only one critical node for collision, node 5 which comes into contact with the fruit and continues colliding.

VI. SIMULATION ANALYSIS

Once a working model of the simulation had been developed, it could now be used to analyze how various simulation
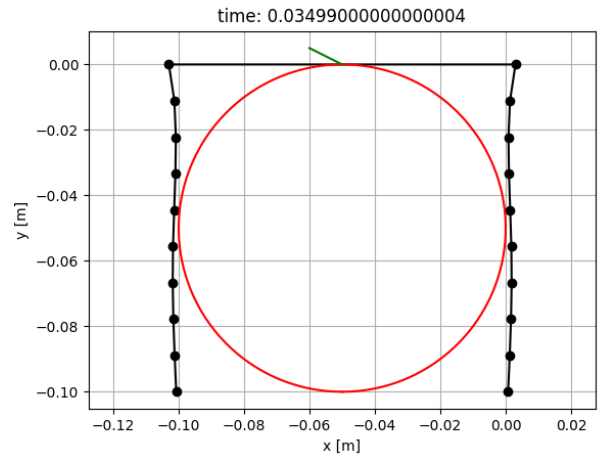

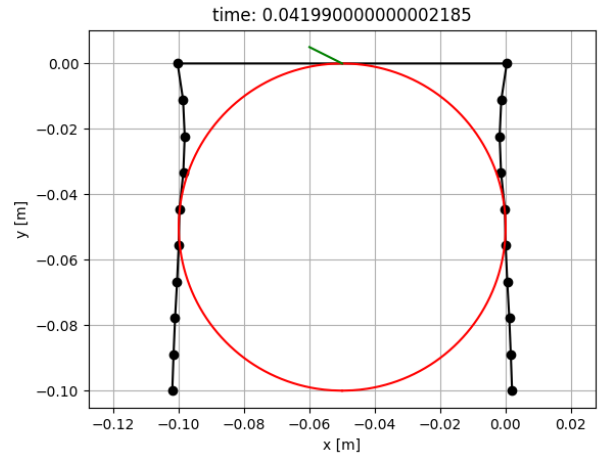Fig. 12: Curved Fruit Implementation 3

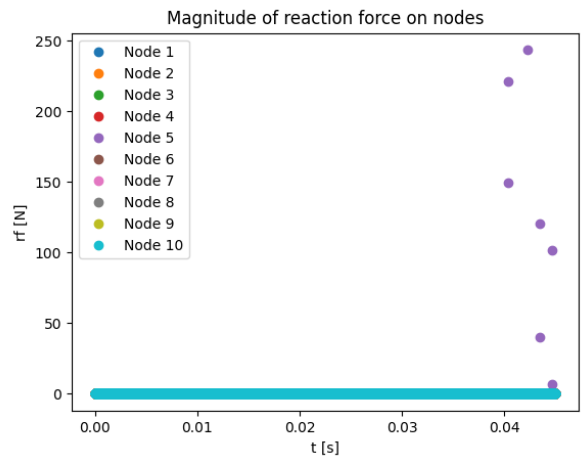
Fig. 13: Curved Fruit Implementation 4

Fig. 14: Reaction Force Magnitude with Curved Surface

parameters affect the outputs. For this analysis, the fruit

radius and the gripper stiffness will be changed to observe how the contact forces and overall model are affected. These parameters were chosen for experimentation as they would influence the design choices in creating a robotic gripper. Further analysis can be done to analyze how other parameters affect results. To analyze how the fruit size affects the model, the radius of the fruit was changed from 5 cm to 4 cm [9]. The resulting plot at a point near contact is shown below. As seen in figure 15, the gripper prongs undergo much more bending as they near contact with the fruit. The collision also takes longer to occur, which influences the increased deformation.
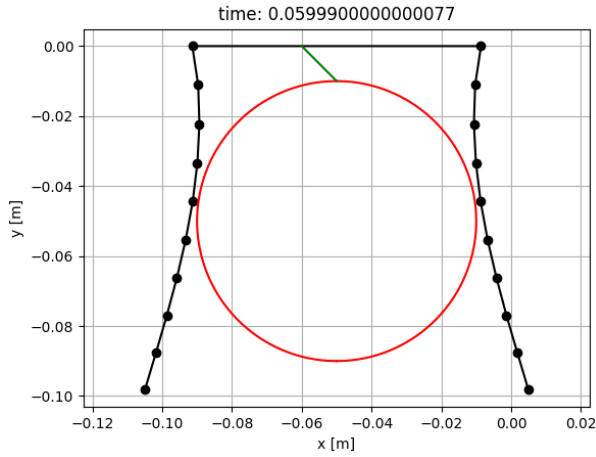

Fig. 15: Simulated Fruit with 4cm Radius

The magnitude of the reaction force for the simulation with a smaller radius is shown below. The maximum reaches 500 N, which is double that from the slightly larger fruit shape. Node 5 is still the critical node, which align with previous results.
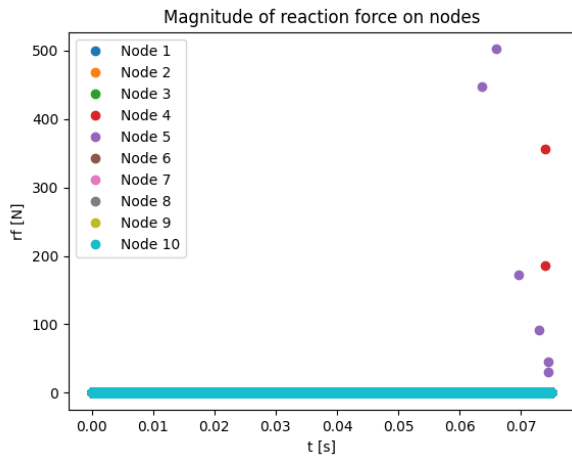

Fig. 16: Reaction Forces Magnitude with 4cm Radius

Similarly, the Young's modulus value of the gripper was altered to test how the material's stiffness influences the results. A Young's Modulus of 1 GPa was used to simulate a soft plastic material such as polyethylene or ABS [10]. As seen in figure 17, the gripper prongs undergo significantly less deformation than those with the lower Young's Modulus. These results align with intuition, as the stiffer material of a plastic would be expected to deform less than a soft rubber material.
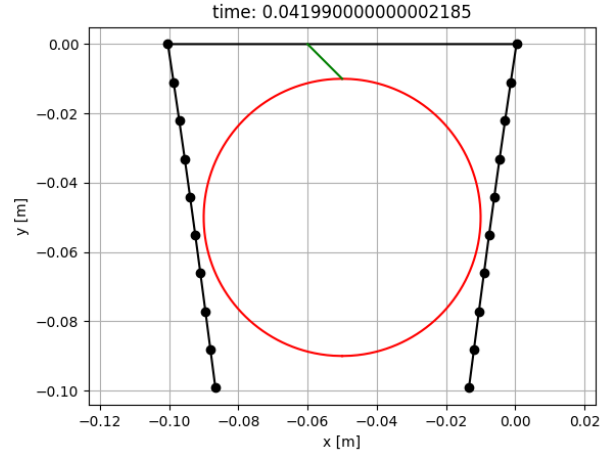

Fig. 17: Simulated Fruit with High Young's Modulus

The magnitude of the reaction force was also increased, with a maximum of 600 N. This is much higher than the maximum for a fruit grasped by rubber prongs. Node 6 was also found to be the critical node and the initial point of contact.
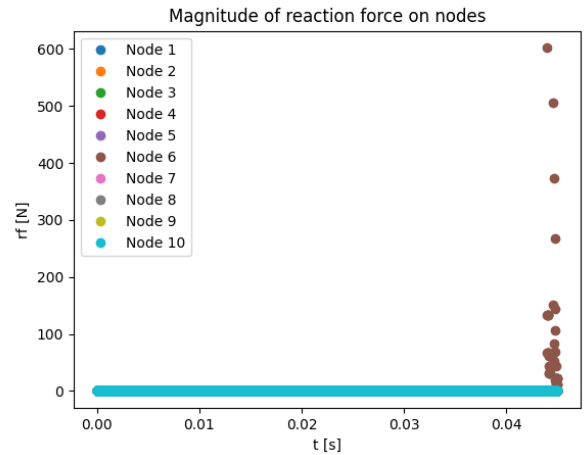

Fig. 18: Reaction Forces Magnitude with High Young's Modulus

VII. PROJECT APPLICATIONS

Within the scope of this project, the modified mass method was used because of the simplification made of contact between a rigid and flexible surface. Within the area of soft robotics, this is particularly useful too because

this simplification can be applied to the materials used within different mechanisms. This project implemented the Modified Mass method within the gripper of an end-effector, but the contact simulation could also be used to simulate structures of robotic arms itself or other links in the system. Modifications could be made to adjust the application location for external forces to then simulate obstacles or actuators present within the soft robot mechanism. Especially within environments containing densely placed obstacles, the Modified Mass method implementation in this project could be applied effectively simulate contact with complex surfaces.

Additionally, the developed simulation could be used to aid in the design of a soft robotic gripper. Different gripper geometries and material properties could be tested in order to select an ideal design based on the desired application and amount of reaction force needed. The fruit collision object could also be replaced with another shape by simply redefining the curvature and calculating the normal vector to the chosen curve. These modifications would allow the current simulation model to be applied for a wide variety of mechanical design and testing.

VIII. CONCLUSIONS

From the proposal, this project was mostly successful in implementing a script to effectively simulate soft grippers within a parallel end-effector. Under the 2D simplifications enforced within the previous sections, this simulation would be applicable for cases involving gripper designs that are symmetric along the geometry's thickness. The calculations within the elastic forces exclude effects of twist, so the simulation for this project would be most representative for fruits, such as apples or kiwis, that practically have rotational symmetry in its geometry.

On the other hand, the following parameters can be changed according to the user's preference:

- Cross sectional area/geometry (Applied uniformly along the gripper length)
- Elasticity
- Simulation time
- Gripper geometry
- Fruit/product location and geometry
- Gripper prong acceleration

With the application of these parameters in this simulation project, one can obtain plots to analyze the reaction forces present from contact with the object to be grasped. Oscillations from contact prevent constant reaction force values, but the frequency of contact and the relative peaks of the reaction force can be interpreted to make design decisions regarding the soft gripper. High magnitudes or high frequency of contact present with a node possibly indicates where critical points in the gripper design would be to analyze with other methods.

The strength of the gripper's material may also be of concern in the grasping process, it also may be of interest to incorporate calculations for internal stresses within

the simulation. While the contact points and corresponding reaction forces indicate potential areas of high stress, the dynamics of the gripper's movement from the end-effector could introduce higher bending stresses at other areas along the geometry. This is possibly due to the sudden changes in acceleration during contact and closer to the constrained points on the end-effectors base. While other software exists to conduct more in-depth finite element method analysis, solving for potential spikes in internal forces would give more information for the user to work with when making design decisions.

As visualization of the dynamics of the grasping method was focus of the project as well, further work may be done to implement more complex control schemes for the end-effector actuation. One might consider cases of rotational movement for the gripper, as this motion is prevalent in existing mechanisms for grasping. As opposed to constant acceleration, varying the acceleration with time could also be considered for the simulation. This would give users another parameter to design for if there are constraints on the geometry or material for the gripper.

Within the simulation method itself, there may be interest to refine the Modified Mass method through implementations for optimal time stepping to collisions. The simulation currently includes varying time-steps upon close proximity with the object, but potentially calculating the exact time-step needed for precise changes in accelerations would give significantly more representative results for the simulation contact. Future iterations of this project would also benefit from implementation in 3D, as imperfections in the fruit surface could introduce significant variations in the contacts in reality as compared to the simulation.

REFERENCES

[1] L. Mu, G. Cui, Y. Liu, Y. Cui, L. Fu, and Y. Gejima, "Design and simulation of an integrated end-effector for picking kiwifruit by robot," *Information Processing in Agriculture*, vol. 7, no. 1, pp. 58–71, 2020. [Online]. Available: https://www.sciencedirect.com/science/article/pii/S2214317318304372

[2] P.-L. Chang, I.-T. Chi, N. D. K. Tran, and D.-A. Wang, "Design and modeling of a compliant gripper with parallel movement of jaws," *Mechanism and Machine Theory*, vol. 152, p. 103942, 2020. [Online]. Available: https://www.sciencedirect.com/science/article/pii/S0094114X20301634

[3] K. Chen, T. Li, T. Yan, F. Xie, Q. Feng, Q. Zhu, and C. Zhao, "A soft gripper design for apple harvesting with force feedback and fruit slip detection," *Agriculture*, vol. 12, no. 11, 2022. [Online]. Available: https://www.mdpi.com/2077-0472/12/11/1802

[4] E. Navas, R. R. Shamshiri, V. Dworak, C. Weltzien, and R. Fernández, "Soft gripper for small fruits harvesting and pick and place operations," *Frontiers in Robotics and AI*, vol. 10, 2024. [Online]. Available: https://www.frontiersin.org/journals/robotics-and-ai/articles/10.3389/frobt.2023.1330496

[5] D. Tong, A. Choi, J. Joo, and M. K. Jawed, "A fully implicit method for robust frictional contact handling in elastic rods," *Extreme Mechanics Letters*, vol. 58, p. 101924, 2023. [Online]. Available: https://www.sciencedirect.com/science/article/pii/S2352431622002000

[6] M. Li, Z. Ferguson, T. Schneider, T. Langlois, D. Zorin, D. Panozzo, C. Jiang, and D. M. Kaufman, "Incremental potential contact: Intersection- and inversion-free large deformation dynamics," *ACM Trans. Graph. (SIGGRAPH)*, vol. 39, no. 4, 2020.

[7] D. Baraff and A. Witkin, "Large steps in cloth simulation," in *Proceedings of the 25th Annual Conference on Computer Graphics and Interactive Techniques*, ser. SIGGRAPH '98. New York,

NY, USA: Association for Computing Machinery, 1998, p. 43–54. [Online]. Available: https://doi.org/10.1145/280814.280821

[8] M. Khalid Jawed and S. Lim, "Discrete simulation of slender structures," 2022.

[9] K. K, A. Tabatabaeefar, M. Hossein, S. Rafiee, A. Sahraroo, A. Rajabipour, and A. Jafari, "Some physical properties of apple," *Pakistan Journal of Nutrition*, vol. 7, 05 2008.

[10] "Chapter 7. polymeric materials," in *Materials For Tribology*, ser. Tribology Series, W. A. Glaeser, Ed. Elsevier, 1992, vol. 20, pp. 177–210. [Online]. Available: https://www.sciencedirect.com/science/article/pii/S0167892208700762